Self-adaptation of manganese–chloride arrangement toward high spin $Mn_5(\mu\text{-}Cl)_4$ cluster-based metal–organic framework with $S = {}^{15}/_{2}$

Shao-Hsuan Lin,[a,b] Chen-I Yang,[a] Ting-Shen Kuo,[b] Ming-Hsi Chiang,[a] Kung-Chung Hsu,[b]* and Kuang-Lieh Lu[a]*

[a] Institute of Chemistry, Academia Sinica, Taipei 115, Taiwan
[b] Department of Chemistry, National Taiwan Normal University, Taipei 116, Taiwan

Synthesis:

A suspension consisting of a mixture of $MnCl_2 \cdot 4H_2O$ (282.5 mg, 1.42 mmol), and Me_3-TBzIm (69.2 mg, 0.135 mmol) in acetone 6 mL and toluene 6 mL was sealed in a Teflon-lined stainless steel vessel (23 mL). The autoclave was placed in an oven maintained at 180 °C for 48 h and then cooled to room temperature at a rate of 3.1 °C/min. The mixture was washed with water and acetone to give yellow block crystals of $\mathbf{1} \cdot 2C_3H_6O$ in a yield of 28% (26.1 mg, 9.36×10^{-3} mmol, based on Me_3-TBzIm). Elemental analysis (%): calcd. for $C_{138}H_{132}Cl_{10}Mn_5N_{24}O_2$ (2787.88): C 59.45, H 4.77, N 12.06; found: C 58.85, H 4.78, N 12.19. IR (KBr, ν_{max}, cm^{-1}): 3387(m), 2347(w), 1751(w), 1614(m), 1509(m), 1479(m), 1463(s), 1393(m), 1290(m), 1229(s), 1197(m), 758(m), 746(s).

X-ray Crystallography. Diffraction measurements for compound $\mathbf{1} \cdot 2C_3H_6O$ were carried out using a Brucker APEXII CCD diffractometer with graphite-monochromated Mo K_α radiation ($\lambda = 0.7107$ Å). Data collation parameters of $\mathbf{1} \cdot 2C_3H_6O$ are listed in Table S1. Structure was solved by direct methods and refined using the SHELXL-97 program[1] by full-matrix least-squares on F^2 values. All non-hydrogen atoms of **1** were refined anisotropically, whereas the hydrogen atoms were placed in ideal, calculated positions, with isotropic thermal parameters riding on their respective carbon atoms. The disordered guest acetone molecule is resolved as a two-sited model using DFIX, FLAT, DELU, SIMU, even ISOR restraint commands to fit actual, severely disordered conditions.

Magnetic measurement. Variable temperature DC magnetic susceptibility measurements were collected on microcrystalline samples, restrained in eicosane to prevent torquing, on a Quantum Design SQUID-VSM magnetometer equipped with a 7.0 Tesla magnet and operating in the range of 1.8–300.0 K. AC magnetic susceptibility were performed on a

Quantum Design PPMS magnetometer. Diamagnetic corrections were estimated from Pascal's constants[3] and subtracted from the experimental susceptibility data to obtain the molar paramagnetic susceptibility of the compounds.

Other Studies. Infrared spectra were recorded in the solid state (KBr pellets) on a Perkin-Elmer PARAGON 1000 FT-IR spectrometer in the 400–4000 cm^{-1} range. Elemental analyses have been carried out by using a Perkin-Elmer TGA-7 TG analyzer.

1. G. M. Sheldrick, *SHELXL-97*; University of Gottingen: Gottingen, Germany, 1997.
2. P. van der Sluis and A. L. Spek, *Acta Crystallogr., Sect. A*, 1990, **46**, 194.
3. E. A. Boudreaux and L. N. Mulay, *Theory and Application of Molecular Paramagnetism*, Wiley J. & Sons, New York, 1976; p. 491.

Detail magnetic analysis

The coupling constants (J) that are strictly required and the spin Hamiltonian are given in eqn 1:

$$H = -2J(S_1S_5 + S_2S_5 + S_3S_5 + S_4S_5) \qquad (1)$$

The Kambe approach for isotropic exchange-coupled systems[4] is a very useful and facile method for yielding energy eigenvalues and eigenvectors; however, entangled exchange paths sometimes prevent the splitting of a whole system into some interacting partial spin sums. An alternative approach, block diagonalization, is available for general isotropic spin systems.[4,5,6] This approach is based on the observation that the HDVV Hamiltonian preserves the z-component of total spin S, $S_Z = \sum_i s_Z(i)$, where $s_Z(i)$ is the z-component of spin on the i-th metal ion in a molecule, owing to the commutation relation $\left[\hat{H}_{\mathrm{HDVV}}, \hat{S}_Z\right] = 0$. For $Mn(II)_5$ complexes, the full matrix dimension is $(2s + 1)^N = 7776$, which is not easily solved. However, the commutation relation allows us to separately solve each block matrix with a different S_Z value and we can confine ourselves to an $S_Z = 1/2$ block matrix with a dimension of only 780, much smaller than the full matrix size. Although a more aggressive reduction in matrix size can be sometimes attempted using the topological symmetry of a molecule, S_Z block matrix diagonalization can be used without any symmetry restrictions and is applicable to general isotropic systems. Starting with decoupled basis vectors, $\left|s_Z(1), s_Z(2), s_Z(3), s_Z(4), s_Z(5)\right\rangle$, the largest block matrix is constructed in the $S_Z = 0$ subspace for integer spin systems. (the $S_Z = -1/2$ subspace should be used for half-odd spin systems). Since the block matrix is much easier to solve than the full matrix, it was diagonalized to provide energy eigenvalues and eigenvectors expressed in terms of decoupled basis vectors. Invoking another commutation relation $\left[\hat{H}_{\mathrm{HDVV}}, \hat{S}^2\right] = 0$, the square of the total spin S^2 is another good quantum number, which we require for labeling an eigenstate along with S_Z. In

order to obtain *S*, the total-spin raising operator ($\hat{S}^{+} = \sum_{i} \hat{s}^{+}(i)$) is evaluated for each eigenvector using $\langle S_Z + 1 | \hat{S}^{+} | S_Z \rangle = \sqrt{(S - S_Z)(S + S_Z + 1)}$, which yields $S = \left| \langle +1/2 | \hat{S}^{+} | -1/2 \rangle \right| - \frac{1}{2}$.

Once the energy eigenvalues $E(S, S_Z)$ are obtained, the van Vleck formula[7] can be used to calculate magnetic susceptibilities as a function of temperature:

$$\chi_m = \frac{N\mu_{\text{eff}}^2}{3k_{\text{B}}T}$$

$$\mu_{\text{eff}}^2 = g^2 \mu_{\text{B}}^2 \sum_{\text{all } S} S(S+1)(2S+1) \exp[-E(S, S_Z)/k_{\text{B}}T] \Big/ \sum_{\text{all } S} (2S+1) \exp[-E(S, S_Z)/k_{\text{B}}T]$$

All of the procedures were coded using the IGOR Pro graphics software package,[8] which is capable of performing non-linear least-squares optimization of a model Hamiltonian.

4. C. Raghu, I. Rudra, D. Sen and S. Ramasesha, *Phys. Rev. B*, 2001, **64**, 064419.
5. N. Regnault, T. Jolicoeur, R. Sessoli, D. Gatteschi and M.Verdaguer, *Phys. Rev. B*, 2002, **66**, 054409.
6. G. Chaboussant, A. Sieber, S. Ochsenbein, H. U. Güdel, M. Murrie, A. Honecker, N. Fukushima and B. Normand, *Phys. Rev. B*, 2004, **70**, 104422.
7. R. L. Carlin, *Magnetochemistry*, Springer-Verlag, Berlin Heidelberg, 1986.
8. IGOR Pro 6, WaveMetrics Inc.

Table S1 Crystallographic data for compound **1**·$2C_3H_6O$.

Empirical formula	$C_{138}H_{132}Cl_{10}Mn_5N_{24}O_2$
Formula weight	2787.88
Temperature	200(2) K
Wavelength	0.71073 Å
Crystal system	Tetragonal
Space group	$P4_2/n$
Unit cell dimensions	a = 22.0951(16) Å
	b = 22.0951(16) Å
	c = 13.0878(11) Å
Volume	6389.4(8) $Å^3$
Z	2
Density (calculated)	1.449 Mg/m^3
Absorption coefficient	0.754 mm^{-1}
F(000)	2878
Crystal size	0.23 × 0.14 × 0.08 mm^3
Theta range for data collection	1.81 to 24.97°
Index ranges	-26<=h<=26, -24<=k<=18, -8<=l<=15
Reflections collected	18245
Independent reflections	5533 [R(int) = 0.0542]
Completeness to θ = 25.00°	98.2 %
Absorption correction	Semi-empirical from equivalents
Refinement method	Full-matrix least-squares on F^2
Data / restraints / parameters	5533 / 54 / 425
Goodness-of-fit on F^2	1.004
Final R indices [$I > 2\sigma(I)$]	R_1[a] = 0.0447, wR_2[b] = 0.0901
R indices (all data)	R_1 = 0.0832, wR_2 = 0.1024
Largest diff. peak and hole	0.377 and -0.349 e.$Å^{-3}$

[a] $R1 = (\Sigma||F_O|-|F_C||)/\Sigma|F_O|$, [b] $wR2 = [\Sigma[w(F_O^2-F_C^2)^2]/\Sigma[w(F_O^2)^2]]^{1/2}$

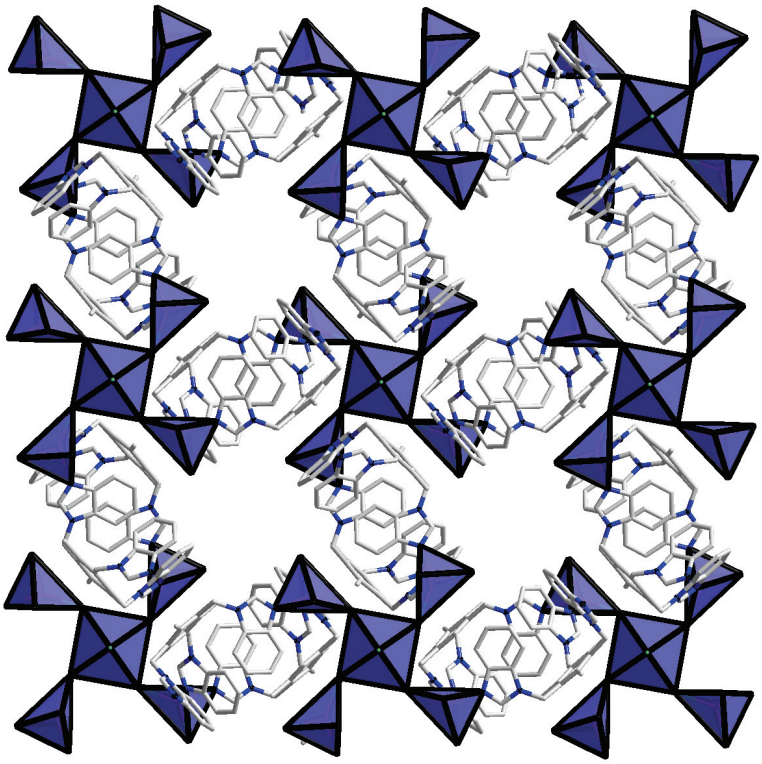

Fig. S1 3D structure of compound **1** viewing along the *c* axis.

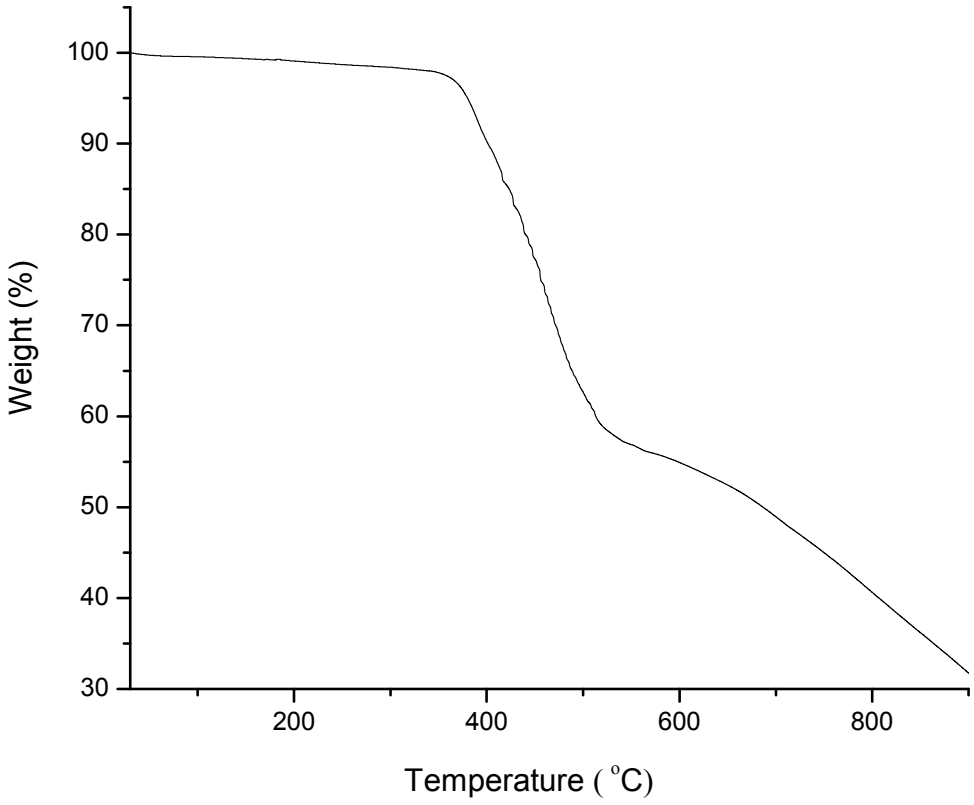

Fig. S2 Thermogravimetric (TG) analysis diagram of **1**.

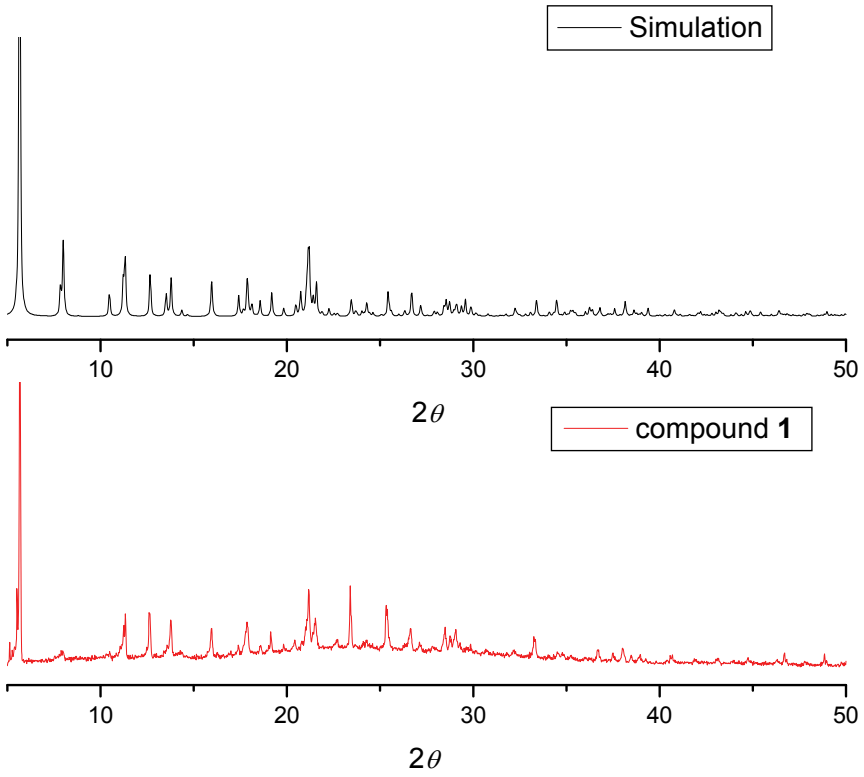

Fig. S3 Simulated PXRD pattern and experimental PXRD pattern of compound **1**.

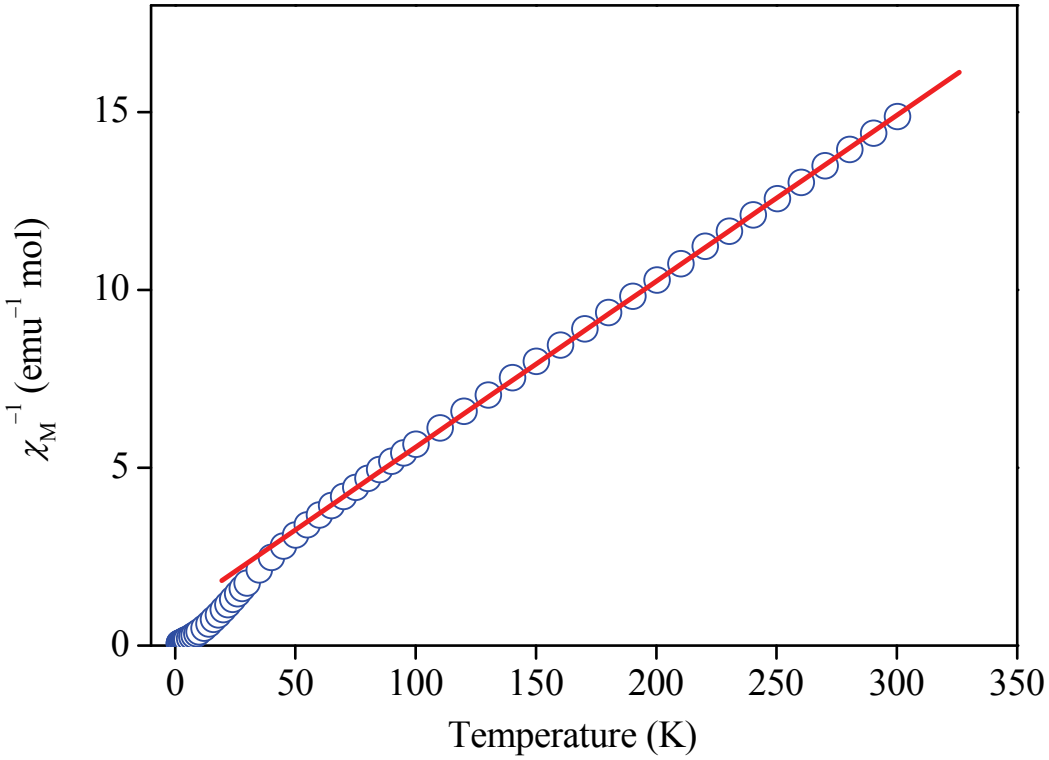

Fig. S4 Plot of χ_M^{-1} (○) vs. temperature for a microcrystalline sample of compound **1**. The solid line represents the best fit χ_M^{-1} above 50 K with a Curie–Weiss law.

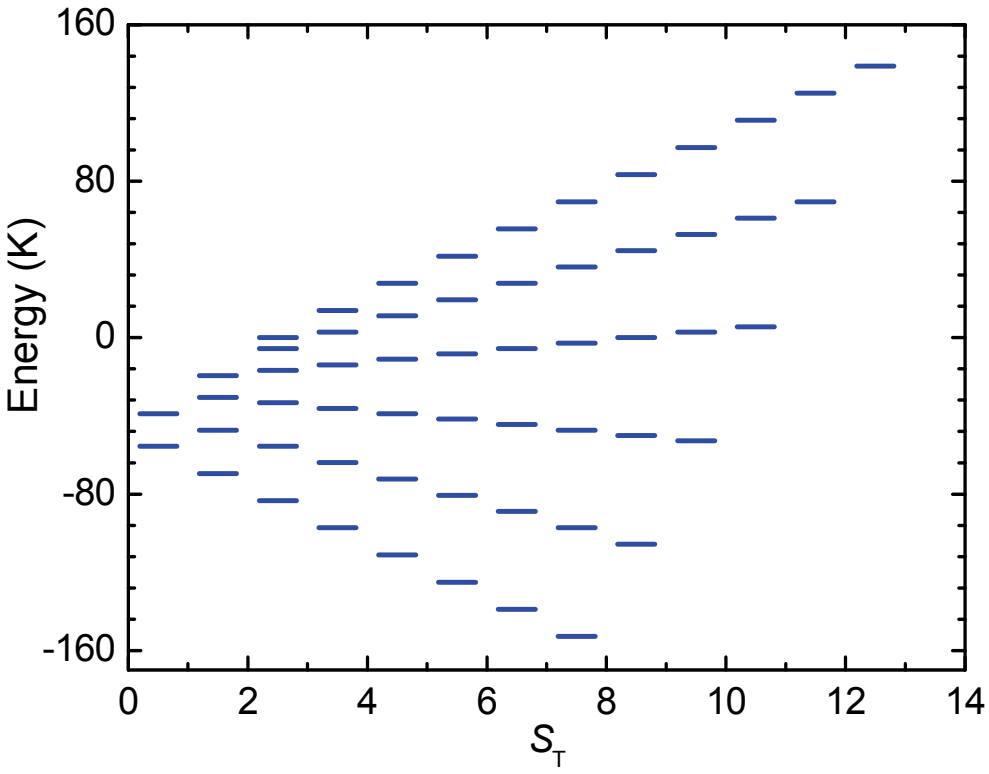

Fig. S5 Diagram of all energy values for all S_T spin states of compound **1**.

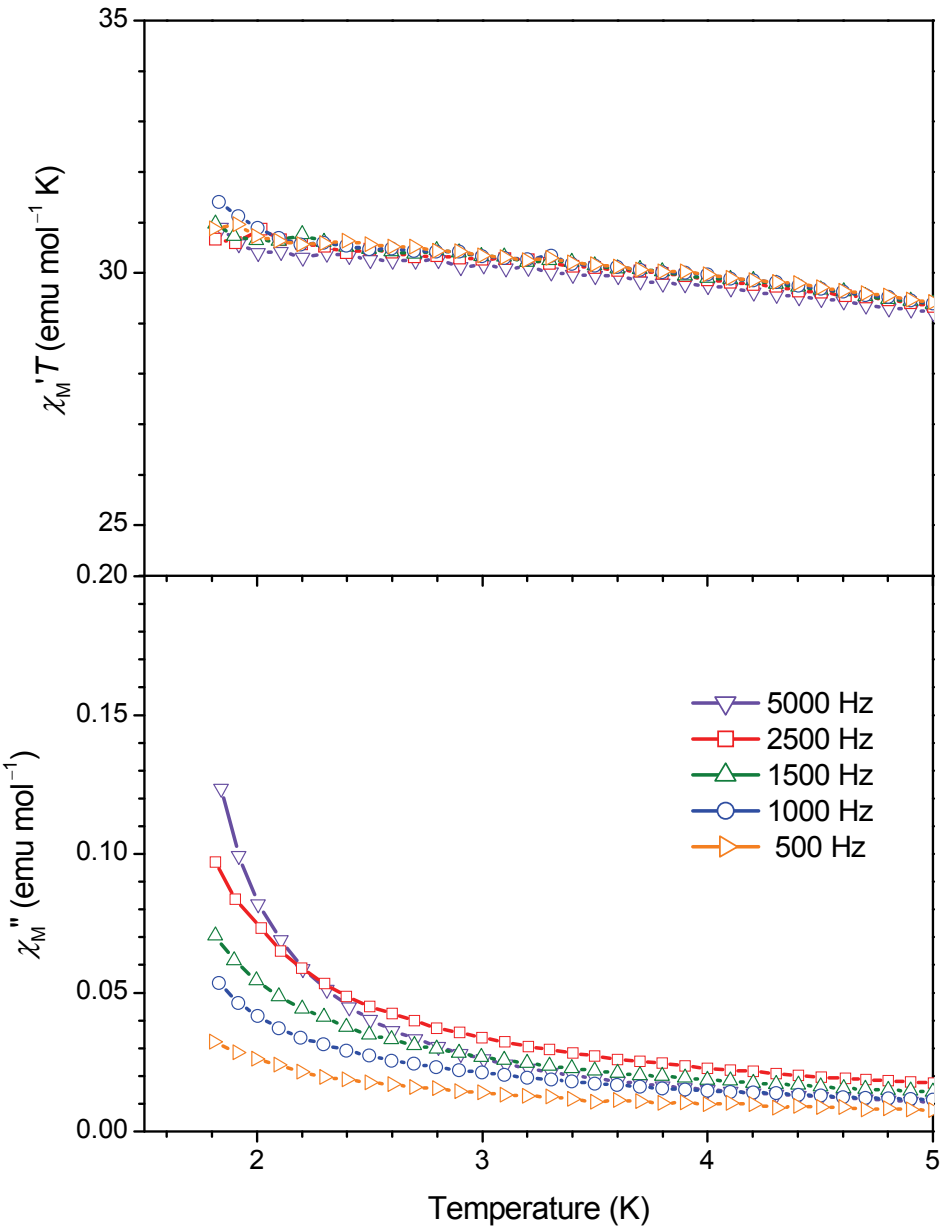

Fig. S6 Plots of $\chi_M'T$ (top) and χ_M'' (bottom) vs. temperature for a microcrystalline sample of compound **1** in a 3.5 G AC field at the indicated frequency.